V European Conference on Computational Fluid Dynamics
ECCOMAS CFD 2010
J. C. F. Pereira and A. Sequeira (Eds)
Lisbon, Portugal, 14–17 June 2010

NUMERICAL AND EXPERIMENTAL ANALYSIS OF THE WIND FORCES ACTING ON LNG CARRIER

A. D. Wnęk*, A. Paço, X-Q. Zhou, C. Guedes Soares

Centre for Marine Technology and Engineering (CENTEC),
Technical University of Lisbon, Instituto Superior Técnico
Av. Rovisco Pais, 1049-001 Lisboa, Portugal
anna.wnek@mar.ist.utl.pt; apaco@mar.ist.utl.pt; qian.zhon@mar.ist.utl.pt;
guedess@mar.ist.utl.pt

Key words: Wind Forces, CFD, LNG ship

Abstract: *The main aim of this work is to present the results of a CFD analysis of the wind forces acting on a LNG ship model and the validation of the numerical model by comparing the results with experimental ones. The numerical analysis was made on a model that was rotated with step of 10 degrees until reproducing the full incidence of 360^o, which corresponds to a series of model tests performed in a wind tunnel. The results are presented in the form of coefficients of the drag and lift force components and yaw moment. A good agreement was obtained between the numerical and experimental results giving confidence in the further use of CFD models similar to these.*

1 INTRODUCTION

Wind usually does not play an important role in ship structure design but it plays a significant role in ship operations such as mooring, towing or positioning. Wind can blow the vessel from any direction and sometimes it can affect the planned trajectory of the ship, in particular at the low speeds that are typical of those maneuvers in which wind effectively decreases her maneuvering capability.

This work is related with a European project, which is addressing the problem of offloading gas from offshore terminals and in particular is studying the problem of the maneuver of a LNG carrier approaching a terminal, which can be a large platform as considered by Wnek et al. [1] or can be another tanker.

The traditional method of determining wind force on ships has been to conduct model tests in wind tunnels. Several compilations of such experimental results have led to the proposal of empirical methods that estimate the wind force coefficients for families of vessels of similar shapes as in the classical works of Isherwood [2] and of Bledermann [3]. Another approach to deal with empirical data is to adopt neural networks models as done by Haddara and Guedes Soares [4].

Over the last several years, Computational Fluid Dynamics (CFD) is becoming more and more widespread as a consequence of better codes and more computational power available. However, before this type of method can be used on its own with appropriate confidence, many validation studies are required to build confidence on the numerical code and on the details of modeling the various types of problems.

Some studies of this type are already available. Yelland et al. [5] estimated the air flow distortion over research ships using both techniques CFD and physical wind tunnel. The air flow simulations were performed at various wind speeds and various wind directions. Popinet et al. [6] showed numerical analysis of the air flow distortion over research vessel for the whole range of wind directions. Main and turbulent characteristics of air flow were compared with experimental dataset. Brizzolara and Rizzuto [7] presented wind pressure field on superstructures geometries of large commercial ships using CFD method. Results were compared with data obtained from formulations based on the stability standards. Kaup [8] described a methodology of CFD analysis of aerodynamic forces acting on a passenger ship. Results in a form of wind coefficients were compared with experimental tests.

Wnek et al. [1] have reported a numerical and experimental analysis of wind loads on floating LNG platform, which followed a similar approach than in the present study. The tested model was rotated in range of wind attack from 0^o to 180^o. Good agreement between CFD and wind tunnel measurements has been achieved.

The present paper describes a numerical analysis of the air flow around a LNG ship model, and the respective assessment of the wind forces calculated by commercial CFD code. The model is from existing ship and the analysis follows the conditions also adopted for the wind tunnel tests. The hull is asymmetrical to the Y axis, which is caused by pipe passage/walk way and cargo machinery/compressor motor room visible on the starboard side of the ship. Thus, to analyze each possible angle of wind blowing, the model was rotated at full incidence of wind attack starting from 0^o on the bow to 350^o with step of 10 degrees. Results of calculations and measurements are presented in terms of coefficients of the drag, lift force components and yaw moment and are compared.

2 NUMERICAL METHOD (CFD)

2.1 Methodology

Numerical prediction of wind loads on LNG model was performed by a Computational Fluid Dynamics tool. The analysis was based on wind tunnel tests using the same model, speed and ship orientations.

The first important step in this method is creating precisely the geometry of the studied ship. Figure 1 represents the virtual LNG carrier, made to reproduce the level of detail that was included in the experimental model. It has been done in Rhinoceros software, wherefore the model was exported to Ansys ICEM CFD software, which was used to produce the required mesh.

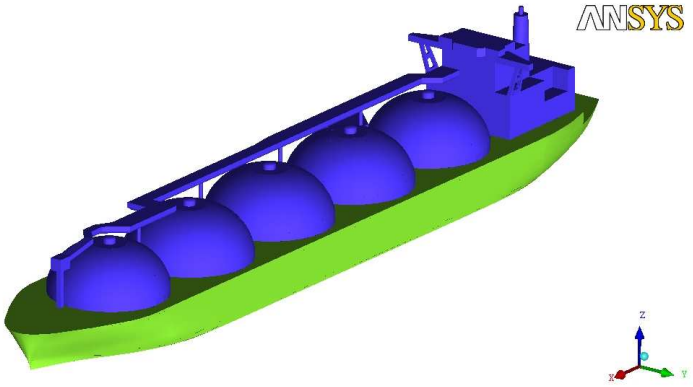

Figure 1. Virtual model of LNG carrier.

Another very important action and often the most time-consuming work in pre-processor is mesh generation. This action needs the suitable computational domain, which in this study was created in a form of a cylinder, shown in Figure 2 with dimensions: H=1.5L and R=3.5L. Thus, there was no need to create separated domains and meshes for each angle of wind attack. Only the inflow and outflow walls were rotating, adopting another position, respectively. The mesh was made of 4 535 517 tetrahedral elements, the majority of which is just by the ship (Figure 3).

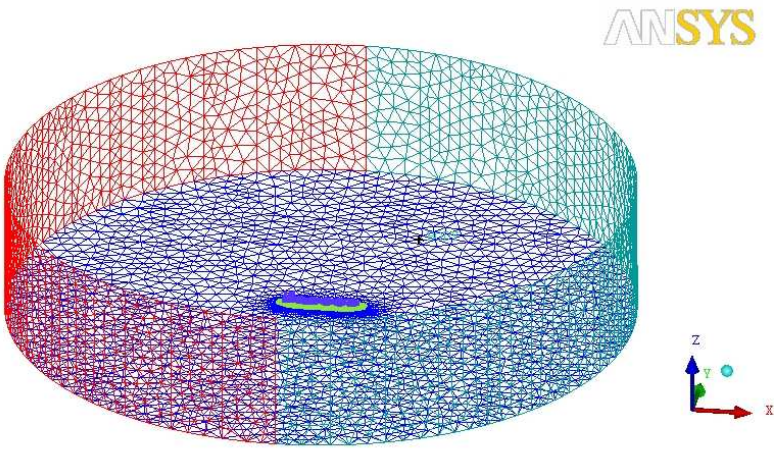

Figure 2. Computational domain.

The estimation of wind loads has been performed by the solver of Ansys CFX using a cluster equipped with Intel® Xeon® CPU E5420 @ 2.50GHz (8 CPUs), 16GB of RAM. Numerical calculations have been made at various angles of wind attack starting from 0^o to 350^o with step of 10 degrees. Before this step, the appropriate boundary conditions were imposed.

Simulation of single phase flow of air with density of 1.2 kg/m^3 was carried out. At the inflow, the average wind velocity components U=10 m/s V=0 m/s W=0 m/s were imposed. The imitation of still water free surface was treated as a free slip wall (no friction on the wall). The top of the domain was far enough away from the model and would not have significant influence on the flow around the ship, that's why it was treated as a symmetry plane. At the outflow, zero pressure was imposed. The no slip condition was applied on the hull of the LNG model, which means wall friction in this case.

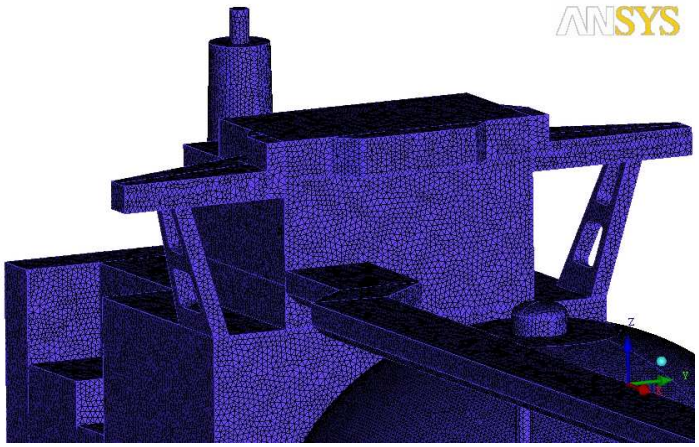

Figure 3. Surface mesh on the hull.

To predict the fluid flow around the ship, the Shear Stress Transport (SST) turbulence model was utilized. The Reynolds number is equal to 4×10^5. The execution of the analysis of each particular flow simulation took about 7 hours.

2.2 Numerical results

The main aim of this work was the validation of CFD model by comparison of the obtained results with those from the wind tunnel. Figure 4 illustrates the wind velocity streamlines for three different angles of wind attack. On the left side, the wind is blowing the portside of the ship, causing big vortices behind the starboard of the vessel. The same phenomenon occurs on the central picture where the wind is blowing fore side of the ship, and the left side figure where the starboard side is attacked by the wind.

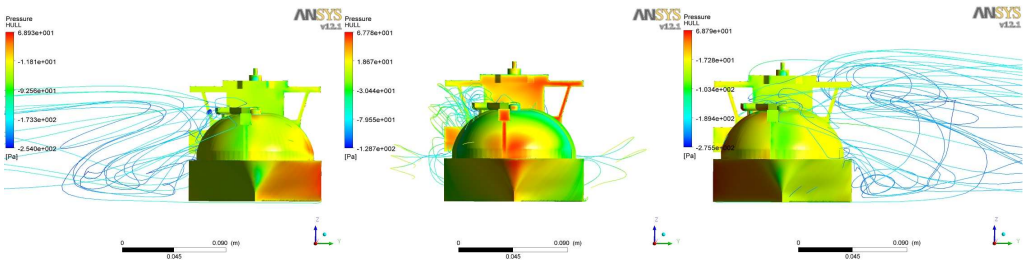

Figure 4. Wind velocity streamlines (angle of incidence: 90^o, 0^o, 270^o)

It is difficult to compare the streamlines between the two cases mentioned (90^o and 270^o), mostly because of asymmetrical grid in relation to the axis Y. However, one can observe that asymmetry against Y axis, which is caused by pipe passage/walk way and cargo machinery/compressor motor room, generates bigger vortices on the starboard side of the ship. Simultaneously, this additional structure affects on different pressure distribution and not equal in magnitude wind loads.

Figure 5 presents the pressure distribution on the model, where the angle of wind attack is 210^o. This is the case which generates the biggest force component F_x in range of full incidence 360^o. The value of longitudinal force coefficient C_x is equal to 0.79, while the opposite side in relation to the axis Y (150^o) gives coefficient equal to 0.76. Comparing lateral force and yaw moment coefficients related to both angles, C_y (210^o) is 1.26 times bigger in magnitude from C_y (150^o) and C_N (210^o) is 1.1 times bigger from C_N (150^o).

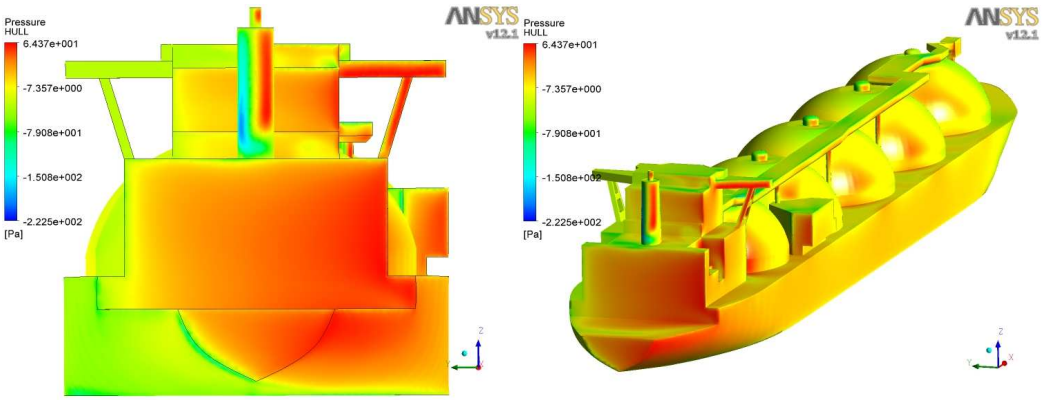

Figure 5. Pressure distribution (angle of incidence 210^o)

Figure 6 represents velocity streamlines together with the vectors of wind attack. The upper figure pictures wind forces blowing the bow of the ship and the lower figure, from the stern of this vessel.

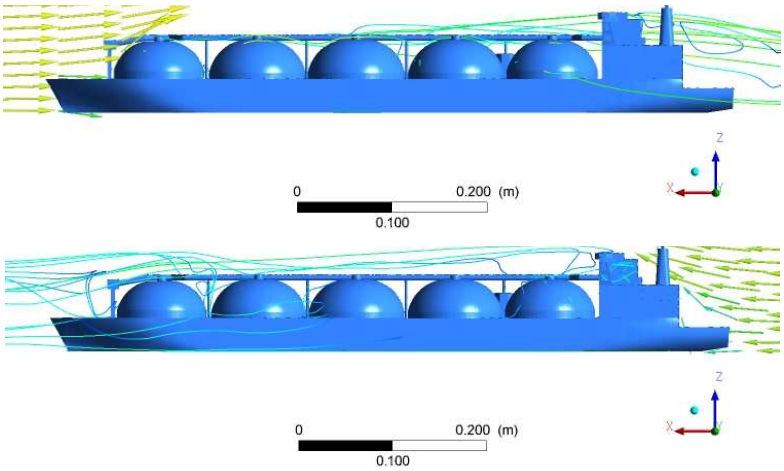

Figure 6. Wind velocity vectors and streamlines (angle of incidence: 0^o, 180^o)

Wind forces, which at the first attack the deckhouse (angle of attack 180^o) cause bigger loads and the vortices around the ship than in the case of 0^o where the smaller in height and width structure (tanks) are attacked by the wind as a first.

3 EXPERIMENTAL METHOD

3.1 Equipment

The experimental tests have been performed in the closed-jet wind tunnel (Figure 7) at Instituto Superior Tecnico in Lisbon, which has a rectangular cross-section and its characteristics are given in the following Table 1.

Cross-section area	1.3×2	m×m
Length of the measurement zone	3	m
Maximum wind speed	15	m/s

Table 1. Wind tunnel characteristics.

Figure 7. IST's closed-jet wind tunnel.

The model of LNG carrier (Figure 8) with five spherical tanks was made of wood and its main characteristics are given in Table 2.

Length overall L_{OA}	0.725	m
Breadth B	0.115	m
Frontal projected area A_F	0.01051	m^2
Lateral projected area A_L	0.05011	m^2

Table 2. LNG models' characteristics.

The model was rotated from 0^o to 350^o with step of 10 degrees. The full incidence 360^o was required by asymmetrical geometry. All tests were performed three times for each orientation by different researchers and on different days so as to allow uncertainty estimates of the measurements.

The results are presented in non-dimensional form as the coefficients of the drag, lift force components and yaw moment:

$$c_x = \frac{F_x}{\frac{1}{2}\rho A_F U^2} \tag{1}$$

$$c_y = \frac{F_y}{\frac{1}{2}\rho A_L U^2} \tag{2}$$

$$c_N = \frac{N}{\frac{1}{2}\rho A_L L_{OA} U^2} \tag{3}$$

Forces F_x, F_y represent components of the drag and lift, which are parallel and perpendicular to model's lateral area, respectively. N represents yaw moment, where the Z axis is positive downwards.

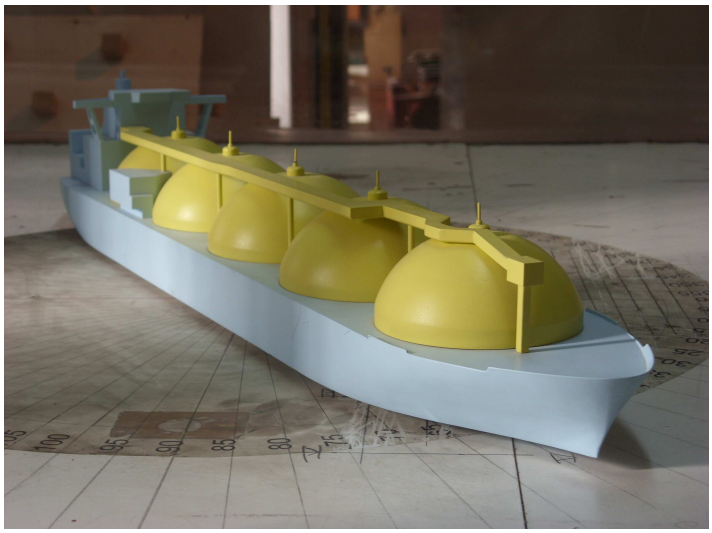

Figure 8. LNG carrier model.

3.2 Experimental results

The experimental tests were performed three times for each angle of attack, denoted by *Test 1, Test 2, Test 3*. Results comparison is shown on the following graphs.

The hull asymmetry is observed already on the first graph (Figure 9), where the forces F_x are bigger in the place of the starboard side of the ship. Likewise, the structure of the vessel causes bigger lateral wind loads, where the wind attacks the starboard side. The maximum lateral force coefficient C_x is almost 1.3 times bigger than on the port side of the ship. Yaw moment is rather symmetrical in magnitude in relation to the Y axis.

There is no significant discrepancy between *Test 1, Test 2* and *Test 3* in this case. However, some deviations, visible mostly on the yaw moment coefficients graph (Figure 5) confirm that repeated experimental tests are never identical; there are always some factors which can perturb experiments. The biggest difference between the same measurements is about 15%.

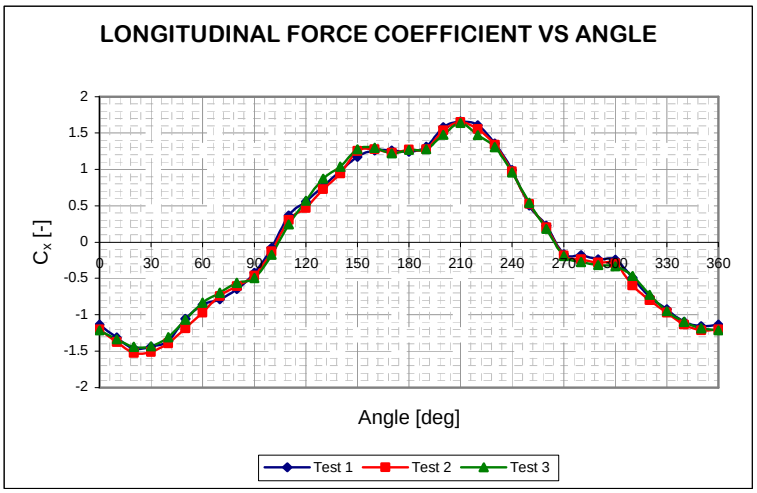

Figure 9. Experimental results of longitudinal force coefficients.

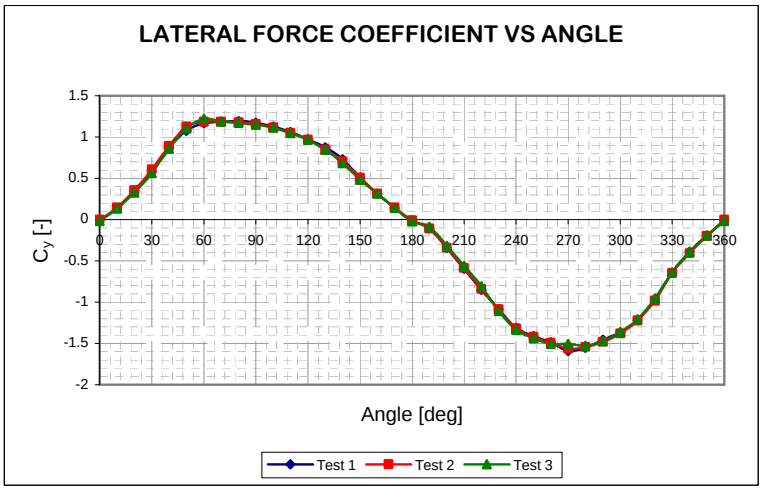

Figure 10. Experimental results of lateral force coefficients.

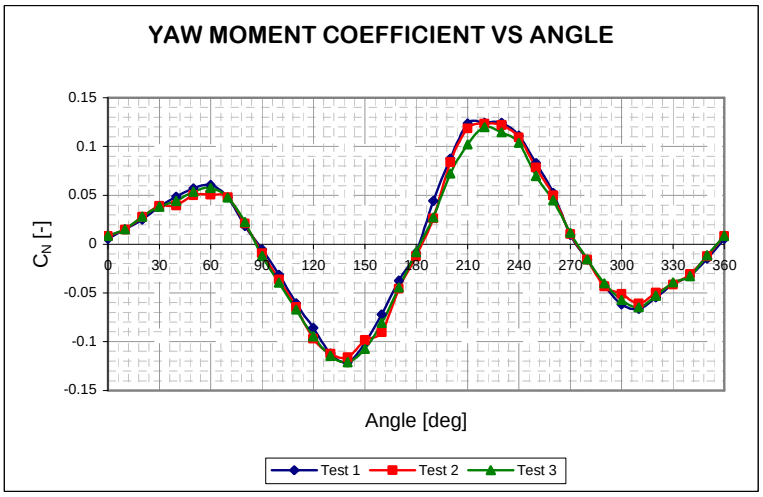

Figure 11. Experimental results of yaw moment coefficients.

4 COMPARISON OF RESULTS

The aim of this work was validation of the CFD model by comparing its results with experimental tests. Numerical and experimental analysis of the wind forces acting on LNG ship model were presented in the previous chapters. This section illustrates the comparisons in the form of coefficients of the drag and lift force components and yaw moment. Analysis of wind loads was performed for full range of incidence 360^o with step of 10 degrees.

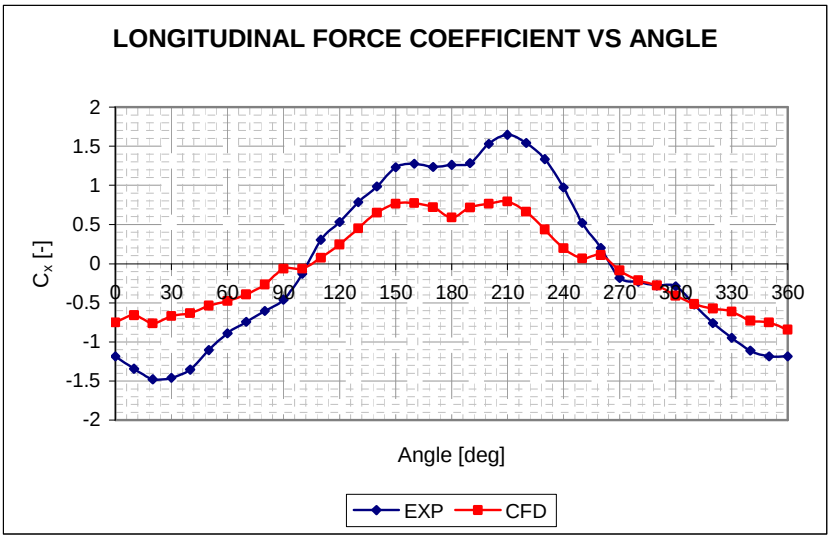

Figure 12. Longitudinal force coefficients C_x.

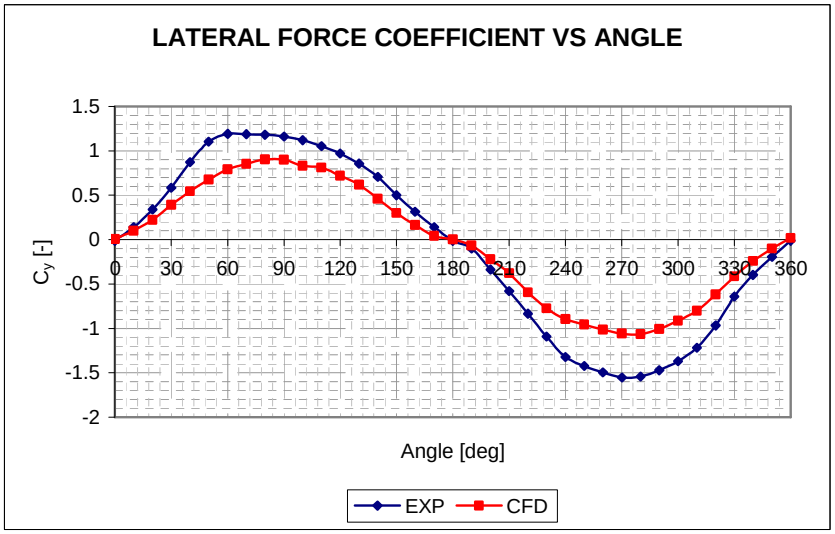

Figure 13. Lateral force coefficients C_y.

Figure 12 presents graphical comparison of longitudinal force coefficients C_x versus angle. CFD results are in a good agreement with experimental measurements related to curves shape. The shape of coefficient curves between CFD and EXP is approximated, which makes the numerical method reliable. However, one can observe, some significant deviations in magnitude between CFD and wind tunnel in place of wind

attack for fore and stern side of the ship. Experimental measurements gave higher values of wind loads than CFD.

Figure 13 illustrates a lateral force coefficients C_y versus angle. In this case, a better agreement between results of numerical and experimental analyses has been achieved. The curves converge well. Maximum deviation appeared for incidence range of 260°-290°.

Very good agreement between CFD and wind tunnel yaw moment coefficients has been achieved, as shown in Figure 14 from where it can be observed that curves almost cover each other.

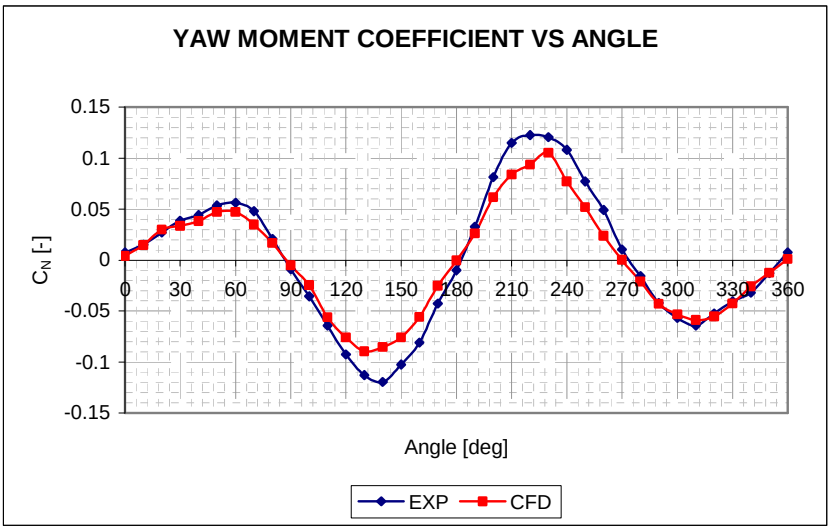

Figure 14. Yaw moment coefficients C_N.

5 CONCLUSIONS

This study has presented the comparison between the wind force coefficients determined by a CFD model with the ones measured in a wind tunnel.

A generally good agreement has been observed, despite not having achieved a perfect match.

For the longitudinal forces the CFD calculations underpredict the measured forces by about 50% despite showing the same dependency on wind direction.

For the lateral forces the same pattern is observed but now the underprediction is only of the order of about 30%.

Better agreement is for the yaw moment coefficient where differences are only of the order of 20% for some angles while for others excellent agreement was obtained.

While from a theoretical point of view all cases are of interest, from a practical perspective the lateral forces (where better agreement was obtained) are more critical for their effect on maneuvering.

ACKNOWLEDGMENTS

The authors are indebted to Dr. Serge Sutulo and Dr. Ricardo Pascoal for their contribution to the overall plan of experiments and to the development of the measuring device.

The paper has been prepared within the project "SAFEOFFLOAD" – Safe Offloading from Floating LNG Platforms", which has been funded by the European Union through the GROWTH program under contract TST4-CT-2005-012560.

REFERENCES

[1] A.D. Wnęk, A. Paço, X-Q. Zhou, C. Guedes Soares, Numerical and experimental analysis of the wind forces acting on a floating LNG platform, In proceedings of the *13th International Congress*, IMAM2009, pp. 697–702 (2009)

[2] R.M. Isherwood, Wind resistance of merchant ships, *Trans. of Roy. Ist. Naval Architects* **114**, pp. 327-338 (1972)

[3] W. Blendermann, Wind Loading of Ships – Collected Data from Wind Tunnel Tests in Uniform Flow, *Institut fur Schiffbau der Universitat Hamburg*, Bericht No 574, pp. 53 (1996)

[4] M.R. Haddara, C. Guedes Soares, Wind loads on marine structures, *Marine Structures* **12**, pp. 199-209 (1999)

[5] M.J. Yelland, B.I. Moat, R.W. Pascal, D.I. Berry, CFD Model Estimates of the Airflow Distortion over Research Ships and the Impact on Momentum Flux Measurements, *Journal of Atmospheric and Oceanic Technology*, pp. 1477-1499 (2002)

[6] S. Popinet, M. Smith, C. Stevens, Experimental and numerical study of the turbulence characteristics of air flow around a research vessel, *Journal of Atmospheric and Oceanic Technology*, pp. 1575-1589 (2004)

[7] S. Brizzolara, E. Rizzuto, Wind Heeling Moments on Very Large Ships. Some Insights through CFD Results, In proceedings of the *9th International Conference of Ships and Ocean Vehicles* (2006)

[8] J. Kaup, Guidelines for Numerical Calculations of Ship Aerodynamic Forces, In proceedings of the *4th International Scientific Conference*, EXPLO-SHIP 2006, Zeszyty Naukowe Nr. 11(83) Akademii Morskiej w Szczecinie, pp. 131-140 (2006)